

We are IntechOpen, the world's leading publisher of Open Access books Built by scientists, for scientists

6,900

Open access books available

186,000

International authors and editors

200M

Downloads

Our authors are among the

154

Countries delivered to

TOP 1%

most cited scientists

12.2%

Contributors from top 500 universities



WEB OF SCIENCE™

Selection of our books indexed in the Book Citation Index
in Web of Science™ Core Collection (BKCI)

Interested in publishing with us?
Contact book.department@intechopen.com

Numbers displayed above are based on latest data collected.
For more information visit www.intechopen.com



Radio Frequency Background

Tales Cleber Pimenta, Paulo C. Crepaldi and Luis H. C. Ferreira
*Universidade Federal de Itajuba
 Brazil*

1. Introduction

Design considerations for the traditional low frequency circuits and the RF circuits are quite different. In low frequency design, the maximum signal transfer occurs when the source presents low impedance while the load presents high impedance. A typical example is a buffer, where the input impedance is high and the output impedance is low. As long as that requirement is fulfilled, the designer is capable of choosing arbitrary levels of impedance that best suits the circuit requirements or applications.

Therefore this chapter aims to provide background on impedance matching between source and load, with or without a transmission line. The analysis can be conducted by using Smith Charts and S-Parameters, which are also presented in this chapter. The analysis in this chapter is oriented to RFID applications whereas other books provide general analysis.

During RF design, the impedances should be matched for maximum signal transfer. Additionally, when the circuits are connected using transmission lines, they should match also the standard values of the transmission lines. At very low frequencies, transmission lines can be thought as just a wire. Nevertheless, at high frequencies, the signal wavelength is comparable to or smaller than the length of the transmissions line and power can be seen as traveling waves. As a matter of fact, even a conductor can be thought as a transmission line in a high frequency circuit.

Most RF equipments and coaxial cables use the standard impedances of 50 or 75 Ω . The value of 75 Ω is used, as an example, in cable TV equipment, since this value provides the minimum losses, as it is desired in transmitting the signal over long distances. In fact, the value of impedance for minimum loss should be 77 Ω , but it was rounded to 75 Ω by convenience.

The value of 50 Ω corresponds to a reasonable compromise, the average, between the minimum loss of a 77 Ω and the maximum power handling capability given of 30 Ω .

2. Transmission line

Fig. 1 shows the lumped component model of a real (lossy) transmission line. The segment indicated corresponds to an infinitesimal segment of the transmission line. The characteristic impedance Z_0 of this line can be found to be [1]:

$$Z_0 = \sqrt{\frac{Z}{Y}} = \sqrt{\frac{R + j\omega L}{G + j\omega C}} \quad (1)$$

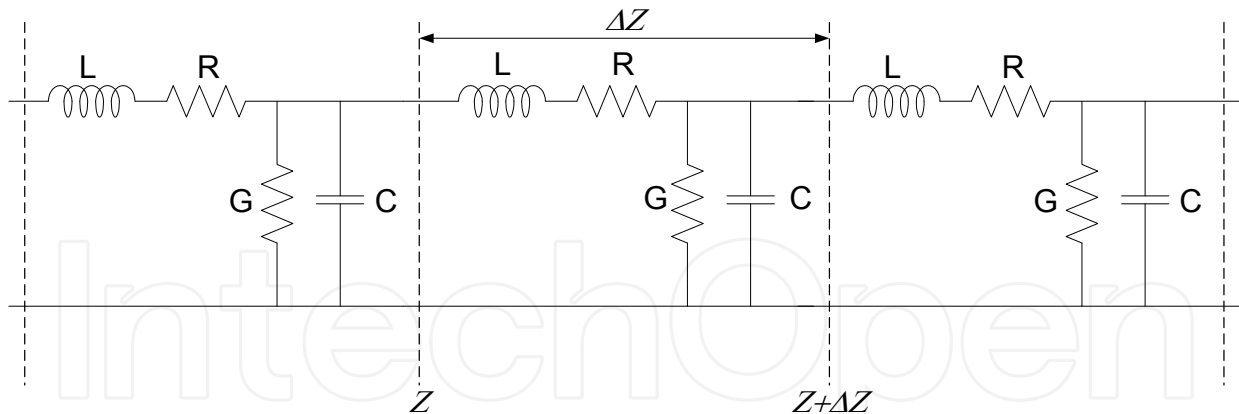


Fig. 1. Lumped component model of a transmission line.

As can be observed, the characteristic impedance Z_0 is dependent on the frequency. Nevertheless, if the resistive terms R and G are negligible, the expression of the characteristic impedance Z_0 can be simplified to:

$$Z_0 = \sqrt{\frac{L}{C}} \quad (2)$$

If the value of RC is equal to GL , expression (1) yields the same value of expression (2). In other words, choosing the L/R time constant of the series impedance equals to the C/G time constant, a lossy line will behave as a lossless line, so that its characteristic impedance will be independent of the frequency[1].

2.1 Reflection coefficient

If a transmission line is terminated by an impedance Z_0 , then a signal traveling down the line with a ratio of voltage to current equal to Z_0 will maintain its ratio upon encountering the load and there will be no reflections. On the other hand, when the load is different of Z_0 , then it imposes its own particular ratio of voltage to current, and the only way to reconcile the conflict is by having some of the signal reflected back towards the source. In order to distinguish the incident and the reflected signals, the subscripts i and r , respectively, will be used.

The incident signal is given by:

$$Z_0 = \frac{E_i}{I_i} \quad (3)$$

At the load end, the mismatch in impedances gives rise to a reflected signal. Since the system is still linear, the total voltage at any point in the system is the sum of incident and reflected voltages. The net current is superposition of incident and reflected currents. However, since the currents are traveling in opposite directions, the net current is the difference between them. Therefore, the load impedance is given by:

$$Z_L = \frac{E_i + E_r}{I_i - I_r} \quad (4)$$

Expression (4) can be rewritten to express Z_L as function of Z_0 as:

$$Z_L = \frac{E_i + E_r}{I_i - I_r} = \frac{E_i}{I_i} \left[\frac{1 + E_r / E_i}{1 - E_r / E_i} \right] = Z_0 \left[\frac{1 + E_r / E_i}{1 - E_r / E_i} \right] \quad (5)$$

The ratio of reflected to incident quantities at the load end of the line is called Reflection Coefficient Γ_L . Therefore, expression (5) can be rewritten as:

$$Z_L = \frac{E_i + E_r}{I_i - I_r} = Z_0 \left[\frac{1 + \Gamma_L}{1 - \Gamma_L} \right] \quad (6)$$

Solving for Γ_L yields:

$$\Gamma_L = \frac{Z_L - Z_0}{Z_L + Z_0} \quad (7)$$

As can be observed from expression (7), if the impedances of the load and the line are equal, there will be no reflection. If the line is terminated in either a short or an open circuit, the reflection will be maximum, with a magnitude of 1 [1].

Therefore, if a transmission line is terminated by its characteristic impedance there will be no reflection since all the transmitted power is absorbed by the load and the energy flows in just one direction.

When the line is terminated by a short circuit a reflected wave is sent back to the source since the short can not sustain any voltage, and therefore dissipates zero power. The incident and the reflected voltage waves are of the same magnitude. They are 180° out of phase at the load and they travel in opposite directions.

If the line is terminated by an open circuit a reflected wave is sent back to the source since the open can not sustain any current, and therefore dissipates zero power. The incident and the reflected current waves are of the same magnitude and travel in opposite directions. The current waves are 180° out of phase at the load, but the incident and reflected voltage waves are in phase [1].

If the line is terminated by an impedance different of the short, open and characteristic impedance, part of the signal will be absorbed by the load and part will be reflected back. The amount of reflected signal is given by expression (7).

3. Smith chart

The reflection coefficient Γ_L of expression (7) was obtained from expression (6). By the same way, solving for Z_L in expression (7) yields Γ_L , thus forming a mapping of one complex number into another. The relationship between these two complex numbers forms a bilinear transformation, which means that knowing one is equivalent to knowing the other.

Since Z_L can have any value and $|\Gamma_L|$ cannot exceed unity for passive loads, it is therefore much more convenient plotting Γ_L than plotting Z_L .

The reflection coefficient can become even more convenient by normalizing it to Z_0 , as:

$$\Gamma = \frac{\frac{Z_L}{Z_0} - 1}{\frac{Z_L}{Z_0} + 1} = \frac{Z - 1}{Z + 1} \quad (8)$$

On the same way, normalizing (6) results in:

$$Z = \frac{1 + \Gamma}{1 - \Gamma} \quad (9)$$

Considering the normalized real and imaginary parts of both Γ and Z then:

$$Z = R + jX = \frac{1 + \Gamma}{1 - \Gamma} = \frac{1 + \Gamma_r + j\Gamma_i}{1 - \Gamma_r - j\Gamma_i} \quad (10)$$

After some algebraic manipulation (using conjugate), the real and imaginary parts are of Z are:

$$R = \frac{1 - \Gamma_r^2 - \Gamma_i^2}{1 + \Gamma_r^2 - 2\Gamma_r + \Gamma_i^2} \quad (11)$$

$$X = \frac{2\Gamma_i}{1 + \Gamma_r^2 - 2\Gamma_r + \Gamma_i^2} \quad (12)$$

Expression (11) can be manipulated as:

$$\begin{aligned} R + R\Gamma_r^2 - 2R\Gamma_r + R\Gamma_i^2 &= 1 - \Gamma_r^2 - \Gamma_i^2 \\ R\Gamma_r^2 - 2R\Gamma_r + R\Gamma_i^2 + \Gamma_r^2 + \Gamma_i^2 &= 1 - R \\ R\Gamma_r^2 - 2R\Gamma_r + R\Gamma_i^2 + \Gamma_r^2 + \Gamma_i^2 &= (1 - R) \frac{(1 + R)}{(1 + R)} \\ R\Gamma_r^2 - 2R\Gamma_r + R\Gamma_i^2 + \Gamma_r^2 + \Gamma_i^2 &= \frac{1}{(1 + R)} - \frac{R^2}{(1 + R)} \\ \Gamma_r^2(1 + R) - 2R\Gamma_r + \frac{R^2}{(1 + R)} + \Gamma_i^2(1 + R) &= \frac{1}{(1 + R)} \\ \Gamma_r^2 - 2\Gamma_r \frac{R}{(R + 1)} + \frac{R^2}{(1 + R)^2} + \Gamma_i^2 &= \frac{1}{(1 + R)^2} \\ \left(\Gamma_r - \frac{R}{R + 1} \right)^2 + \Gamma_i^2 &= \left(\frac{1}{1 + R} \right)^2 \end{aligned} \quad (13)$$

Similarly, expression (12) into:

$$\left(\Gamma_r - 1 \right)^2 + \left(\Gamma_i - \frac{1}{X} \right)^2 = \frac{1}{X^2} \quad (14)$$

When the two parametric equations (13) and (14) are drawn on a complex coordinate, they build the Smithchart. Equation (13) forms resistance circles, and equation (14) generates reactance circles, as shown in Fig. 2 and Fig. 3, respectively. The resulting Smithchart is illustrated in Fig. 4.

As can be verified from expression (13), the imaginary axis in the Z -plane (resistance equals 0) is mapped as a unity circles into Γ -plane. The other lines of constant resistance in the Z -plane are also mapped as circles, but of different diameter in the Γ -plane. Nevertheless, they

are all tangent at the point $\Gamma=1$, as shown in Fig. 2. The larger the value of the resistance, the smaller becomes the circle [1, 2].

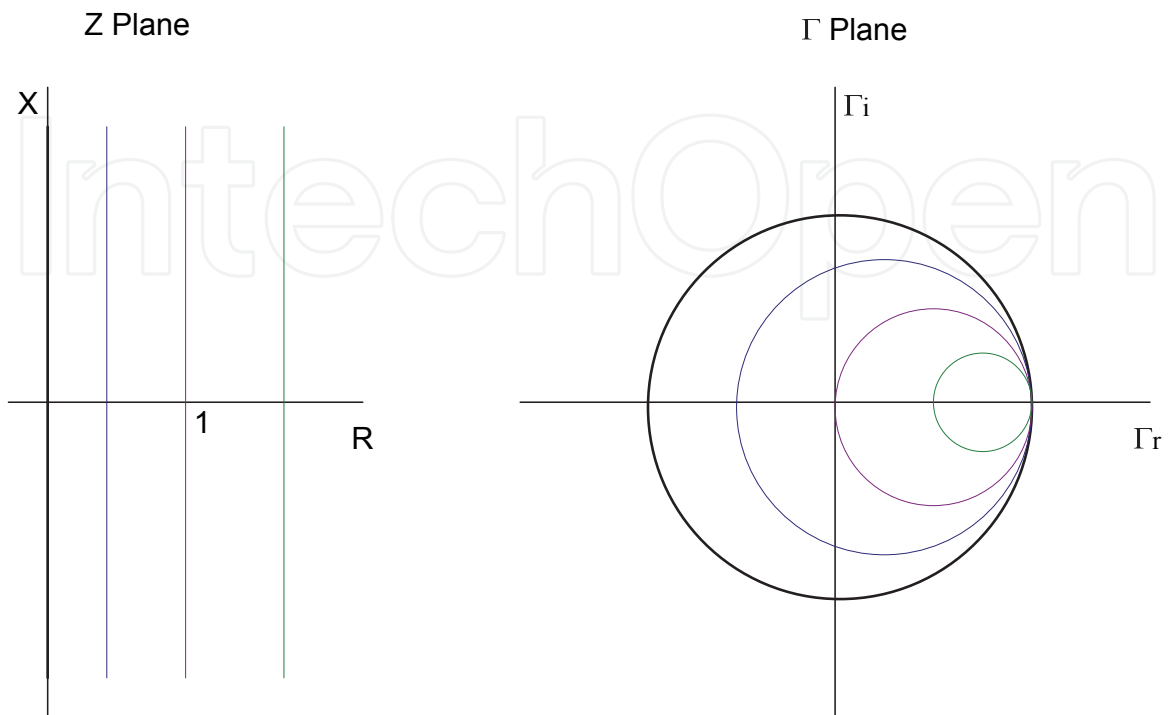


Fig. 2. Mapping of Z-plane into Γ -plane for constant resistances.

As can be verified from expression (14), lines of constant reactance are perpendicular to lines of constant resistance in the Z-plane. This same orthogonality is preserved in the Γ -plane by having arcs perpendicular to the constant resistance lines, as indicated in Fig. 3.

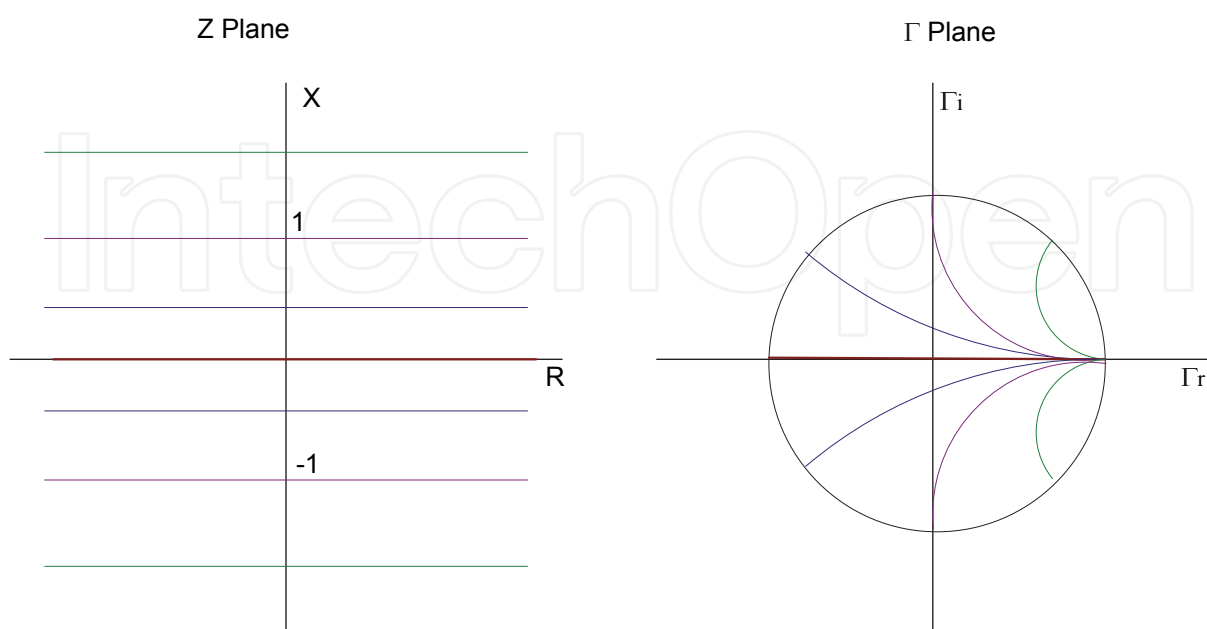


Fig. 3. Mapping of Z-plane into Γ -plane for constant reactances.

The Smith, as shown in Fig. 4, is just the plotting of both constant resistance and constant reactance, but without the presence of the Γ axes. The center of the Smith chart corresponds to zero reflection (Z_L equals Z_0)[1].

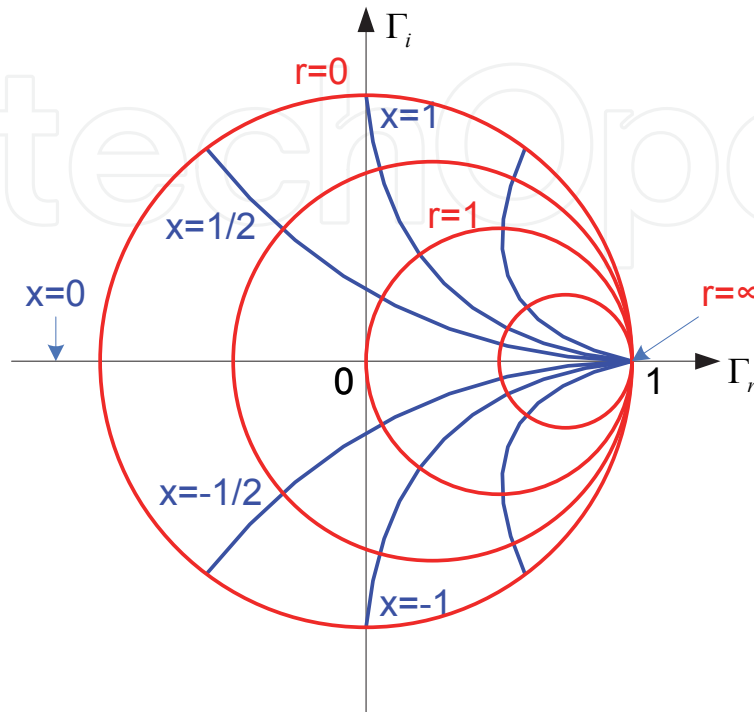


Fig. 4. Smith chart.

The upper half of the Smith chart corresponds to the upper half part of the Z -plane, and therefore presents inductive loads. On the same way, the bottom half of the Smith chart corresponds to the bottom half part of the Z -plane, thus representing capacitive loads. Obviously, the Re axis of the Smith chart represents purely resistive loads.

Although the Smith chart presents many interesting and useful properties, they will not be presented here due to the focus of this material.

2.1 Admittance chart

The Smithchart is built by considering impedance (resistance and reactance). Once the Smithchart is developed, a similar approach can be used for admittance analysis. The concept that admittance is the inverse of impedance is very important for parallel circuit synthesis. Adding new elements in series can be resolved easily by adding the impedance values. However, summing elements in parallel can be cumbersome in terms of impedance. Thus, admittance is often considered for parallel elements.

By definition, admittance is expressed as:

$$Y = \frac{1}{Z} = G + jB \quad (15)$$

where G is conductance and B is susceptance of the element. The reflection coefficient Γ can be expressed in terms of normalized admittance as:

$$\Gamma = \Gamma_r + j\Gamma_i = \frac{Z_L - Z_0}{Z_L + Z_0} = \frac{\frac{1}{Y_L} - \frac{1}{Y_0}}{\frac{1}{Y_L} + \frac{1}{Y_0}} = \frac{Y_0 - Y_L}{Y_0 + Y_L} = \frac{1 - y}{1 + y} = \frac{1 - g - jb}{1 + g + jb} \quad (16)$$

The admittance reflection coefficient $\Gamma(y)$ is given by definition as:

$$\Gamma(y) = \frac{Y_L - Y_0}{Y_L + Y_0} \quad (17)$$

As can be observed, the value of the admittance reflection coefficient $\Gamma(y)$ is equal to $-\Gamma$, the reflection coefficient in terms of impedance. Therefore, once Γ is known, $\Gamma(y)$ can be located a point at the same distance from the origin. Rotating the admittance point by 180° around the origin achieves the same result.

The admittance Smithchart can be obtained using the same procedure used to construct the impedance Smithchart. The normalized real and imaginary parts of Γ and Y can be given as:

$$Y = G + jB = \frac{1 - \Gamma_r^2 - \Gamma_i^2 - j2\Gamma_i}{1 + \Gamma_r^2 + 2\Gamma_r\Gamma_i + \Gamma_i^2} \quad (18)$$

After some algebraic manipulation (using conjugate), the real and imaginary parts are of Y are:

$$G = \frac{1 - \Gamma_r^2 - \Gamma_i^2}{1 + \Gamma_r^2 + 2\Gamma_r\Gamma_i + \Gamma_i^2} \quad (19)$$

$$B = \frac{-2\Gamma_i}{1 + \Gamma_r^2 + 2\Gamma_r\Gamma_i + \Gamma_i^2} \quad (20)$$

Using the same procedure presented for expressions (13) and (14), then the parametric equations of the admittance Smithchart are:

$$\left(\Gamma_r + \frac{G}{G+1}\right)^2 + \Gamma_i^2 = \left(\frac{1}{1+G}\right)^2 \quad (21)$$

$$(\Gamma_r + 1)^2 + \left(\Gamma_i + \frac{1}{B}\right)^2 = \frac{1}{B^2} \quad (22)$$

When the two parametric equations (21) and (22) are drawn on a complex coordinate, they build the Admittance Smithchart. Equation (21) forms resistance circles, and equation (22) generates reactance circles, as shown in Fig. 5.

3. S Parameters

At low frequencies, linear systems can be analyzed by means of voltages and currents applied to its ports. The two port circuit shown in Fig. 5 could be analyzed from its

impedance (Z-parameters), admittance (Y-parameters), or a mixture of them, which could be hybrid (H-parameters) and inverse-hybrid (G-parameters).

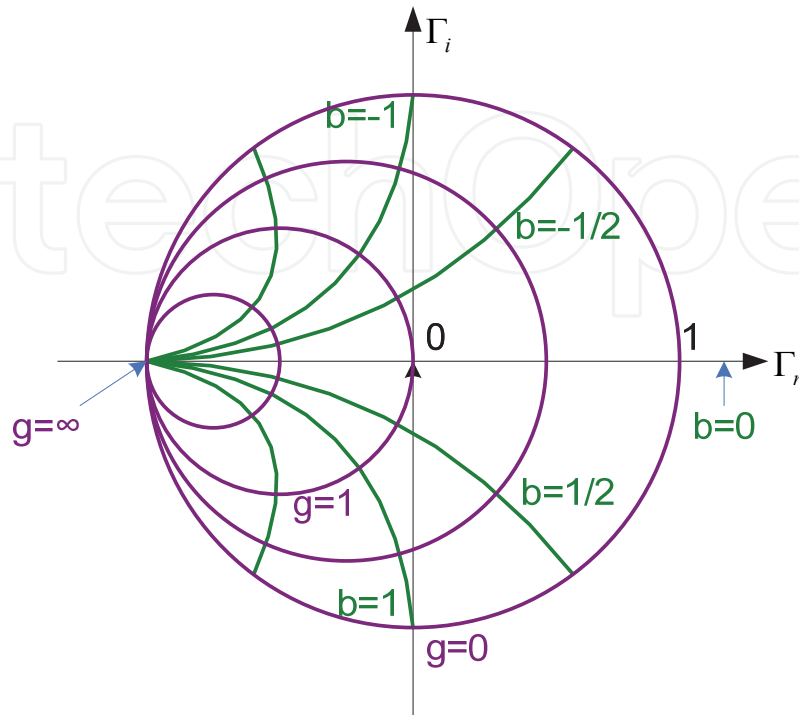


Fig. 5. Admittance Smithchart.

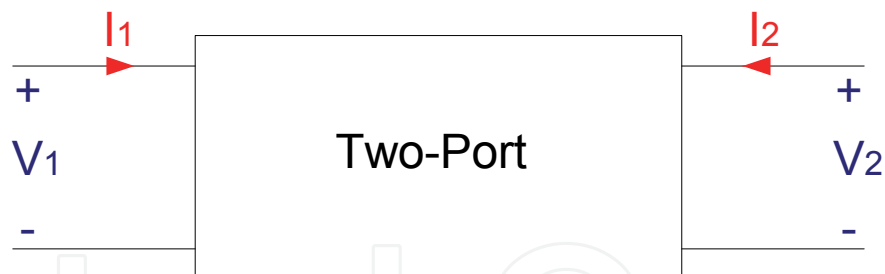


Fig. 6. Two port circuit representation.

As an example, the circuit of Fig. 5 could be analyzed using H parameters whose equations are:

$$\begin{aligned} V_1 &= h_{11}I_1 + h_{12}V_2 \\ I_2 &= h_{21}I_1 + h_{22}V_2 \end{aligned} \quad (16)$$

As can be observed from the equations, the value of h_{11} (port 1 impedance) can be obtained directly from the relationship of V_1 and I_1 when V_2 is set to zero. A voltage source is set to zero by shortening its terminals. The value of h_{21} (current gain from port 1 to port 2) is obtained from the relationship of I_1 and I_2 also when V_2 is set to zero.

By the same way, h_{12} (voltage gain from port 2 to port 1) can be obtained from the relationship of V_1 and V_2 when I_1 is set to zero. A current source is set to zero by opening its

terminals. Finally, h_{21} (port 2 conductance) is obtained from the relationship of V_2 and I_2 when I_1 is set to zero.

Shorting or opening terminals is feasible at low frequencies but virtually impossible at high frequencies, particularly over a broad range of frequencies. Additionally, RF circuits are very sensitive to impedances, and they may oscillate or just quit working when terminated with open or short circuits. Therefore, Z-parameters, Y-parameters, H-parameters and G-parameters are not suitable to high frequency operations.

For high frequency operations, the *scattering* parameters (or just S-parameters) are employed. The input and output variables in S-parameters are based on incident and reflected voltage waves instead of voltages and currents.

The S-parameters takes advantage of the fact that there is no reflection in a line terminated in its characteristic impedance. Therefore, it is necessary a circuit representation for S-parameters, where source and the load terminations are Z_0 , as shown in Fig. 6.

The S-parameters equations are:

$$\begin{aligned} b_1 &= s_{11}a_1 + s_{12}a_2 \\ b_2 &= s_{21}a_1 + s_{22}a_2 \end{aligned} \quad (16)$$

where

$$\begin{aligned} a_1 &= E_{i1} / \sqrt{Z_0} \\ a_2 &= E_{i2} / \sqrt{Z_0} \\ b_1 &= E_{r1} / \sqrt{Z_0} \\ b_2 &= E_{r2} / \sqrt{Z_0} \end{aligned} \quad (17)$$

The normalization by $\sqrt{Z_0}$ is very convenient since the square of a and b corresponds to the power of the incident and reflected waves.

S_{11} and S_{21} can be obtained by measuring the incident, the reflected and the transmitted signals at the input when the output is terminated in Z_0 . Once the output is terminated by Z_0 there is no reflection. The values of S_{11} and S_{21} are:

$$\begin{aligned} S_{11} &= \frac{b_1}{a_1} = \frac{E_{r1}}{E_{i1}} = \Gamma_1 \\ S_{21} &= \frac{b_2}{a_1} = \frac{E_{r2}}{E_{i1}} \end{aligned} \quad (18)$$

Similarly, S_{12} and S_{22} can be obtained by measuring the incident, the reflected and the transmitted signals at the output when the input is terminated in Z_0 . Since the input is terminated by Z_0 there is no reflection. The values of S_{12} and S_{22} are:

$$\begin{aligned} S_{12} &= \frac{b_1}{a_2} = \frac{E_{r1}}{E_{r2}} \\ S_{22} &= \frac{b_2}{a_2} = \frac{E_{r2}}{E_{i2}} = \Gamma_2 \end{aligned} \quad (19)$$

S_{11} corresponds to the input reflection coefficient, S_{21} is the input to output (direct) gain, S_{12} is the reverse transmission gain and S_{22} corresponds to the output reflection coefficient. The magnitudes of S_{11} and S_{22} are always less than 1, where a value of zero represents a perfect matching (no reflections), and the closer to 1, the higher the reflection. The magnitudes of S_{21} (transfer characteristic) and S_{12} (reverse) are smaller than 1 for passive circuits but can exceed 1 for active circuits (amplification). A positive value means the input and output signal are in phase and a negative indicates a phase shift.



Fig. 7. Two port circuit representation for S-parameters.

3.1 Measurements of S-Parameters

The circuit topology used to measure S-Parameters is given in Fig. 7.



Fig. 8. Circuit topology used to measure S-Parameters.

The input reflection coefficient S_{11} from expression (18) can be modified as:

$$S_{11} = \Gamma_1 = \frac{Z_L - Z_0}{Z_L + Z_0} = 2 \cdot \frac{Z_L}{Z_L + Z_0} - 1 \quad (20)$$

This expression, using the concepts of voltage division, corresponds to:

$$S_{11} = \Gamma_1 = 2 \cdot \frac{Z_L}{Z_L + Z_0} - 1 = 2 \cdot \frac{V_1}{V_S} - 1 \quad (21)$$

Here, Z_L corresponds to the input impedance of the two-port circuit. The value of the input to output gain, S_{21} is given as:

$$S_{21} = 2 \cdot \frac{V_2}{V_S} \quad (22)$$

The value of S_{22} and S_{12} can be obtained in a similar way by just exchanging input and output terminals.

3.1 S Parameters in the Smith chart

The center point of the Smith chart corresponds to the point of zero reflection, where Z_L equals Z_0 . Plots of S_{11} and S_{22} on the real axis represent ohmic resistors, above the axis indicate inductive load while below the axis indicate capacitive loads.

Plots of S_{12} and S_{21} inside the Smith chart indicate that damping signal between ports, whereas plots outside the chart indicate amplification [1].

As the frequency increases, the S-Parameters plots in the Smith chart move clockwise.

Given the value of S_{11} , the circuit impedance can be found from (6), as:

$$Z_L = Z_0 \left[\frac{1 + S_{11}}{1 - S_{11}} \right] \quad (23)$$

3.2 Application example

The S_{11} and S_{21} parameters can be obtained as given by expressions (21) and (22), indicated in Fig. 7, and the values are calculated as for S_{11} and S_{21} , respectively. As an application example, consider the cascode amplifier shown in Fig. 8 [2].

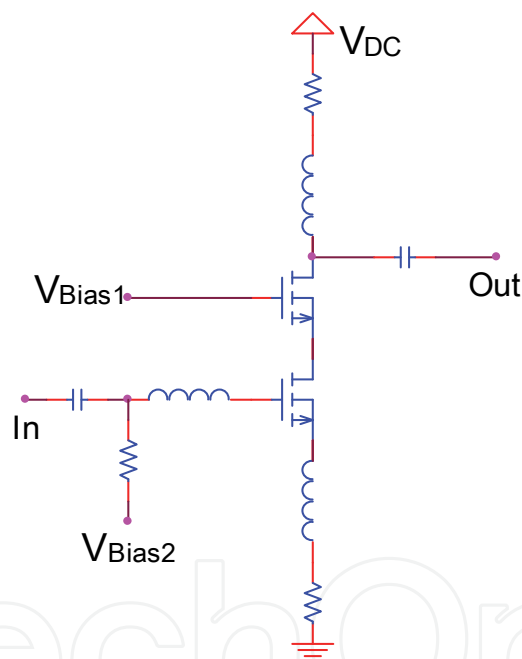


Fig. 9. Cascode amplifier.

Fig. 10 shows its S_{11} parameter, in the Smith chart. The frequency is ranging from 4GHz to 6GHz. As the frequency increases, the plot moves clockwise. At approximately 5GHz, the circuit presents a pure resistive impedance of approximately 50Ω (it crosses the horizontal axis). The circuit presents a capacitive behavior for frequencies below 5GHz and an inductive behavior for higher frequencies [1].

The same parameters could be plotted in a standard dB format, as shown in Fig. 11. The graph of Fig. 10 provides more information and insight than the graph of Fig. 11. The last one provides only the magnitude, whereas the first one provides both the imaginary and real part, so that it is possible to infer a capacitive and/or inductive behavior of the circuit, among other information.

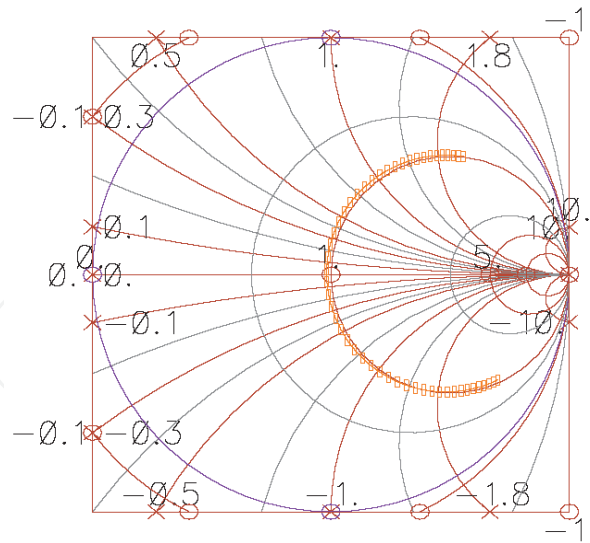


Fig. 10. S_{11} parameter of the circuit from Fig. 8, in a Smith chart.

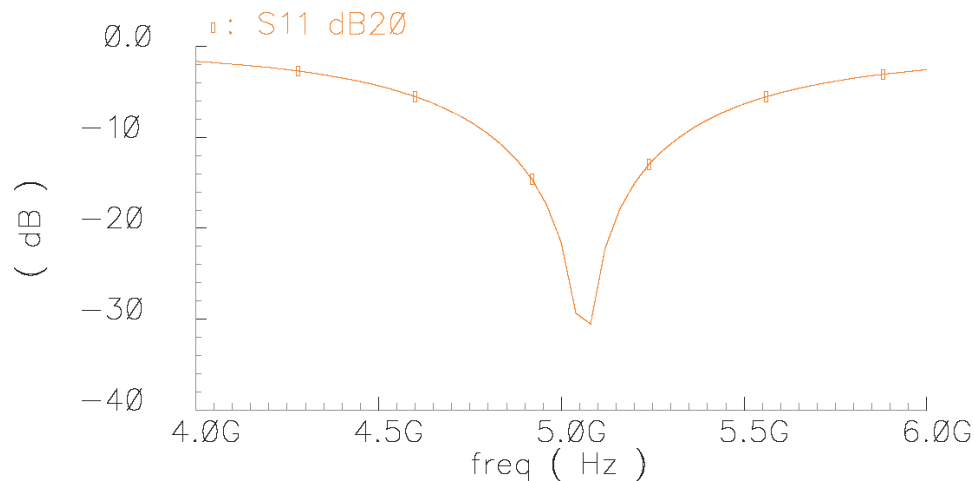


Fig. 11. S_{11} parameter of the circuit from Fig. 8, in a dB chart.

Unfortunately, it is not always possible to analyze S-parameters using Smith chart. One such case is S_{11} that is usually larger than 1 for active circuits. If it is larger than one, it does not fit the Smith chart!

4. Noise figure/factor

In analog circuits at low frequency, the signal-to-noise figure (SNR), defined as the ratio of signal power to the noise power, is an important and very used parameter. As an example, in a radio receiver, it indicates the quality of the demodulated signal [2-5].

Nevertheless, as the signal passes through the RF circuits, the SNR changes. This signal-to-noise degradation along the system is described by the noise factor (F), as:

$$F = \frac{SNR_i}{SNR_o} = \frac{S_i/N_i}{S_o/N_o} \quad (24)$$

where the index i refers to input and the index o refers to output.

If a system has no noise, then $SNR_o = SNR_i$ regardless of the gain, and $F=1$. This would be case of a hypothetical noiseless amplifier. Therefore, the noise figure of a real system will be always larger than 1.

Considering A as the system gain, expression (24) can be modified to:

$$F = \frac{S_i/N_i}{S_o/N_o} = \frac{S_i/N_i}{S_i \cdot A/N_o} = \frac{N_o}{A \cdot N_i} \quad (25)$$

which can be seen as the total output noise power over the output noise due to the input source.

The total output noise is the sum of the original noise at the input (which was amplified) and the noise added by the circuit. This can be denoted as:

$$N_o = A \cdot N_i + N_{added} \quad (26)$$

Therefore, expression (18) can be expressed also as:

$$F = \frac{N_o}{A \cdot N_i} = \frac{A \cdot N_i + N_{added}}{A \cdot N_i} = 1 + \frac{N_{added}}{A \cdot N_i} \quad (27)$$

Again, if the circuit adds no noise, F becomes 1.

Another important figure of merit is the noise figure, NF , expressed as:

$$NF = 10 \cdot \log_{10} F \quad (28)$$

While the noise factor of a noiseless circuit is 1, the noise figure is 0dB.

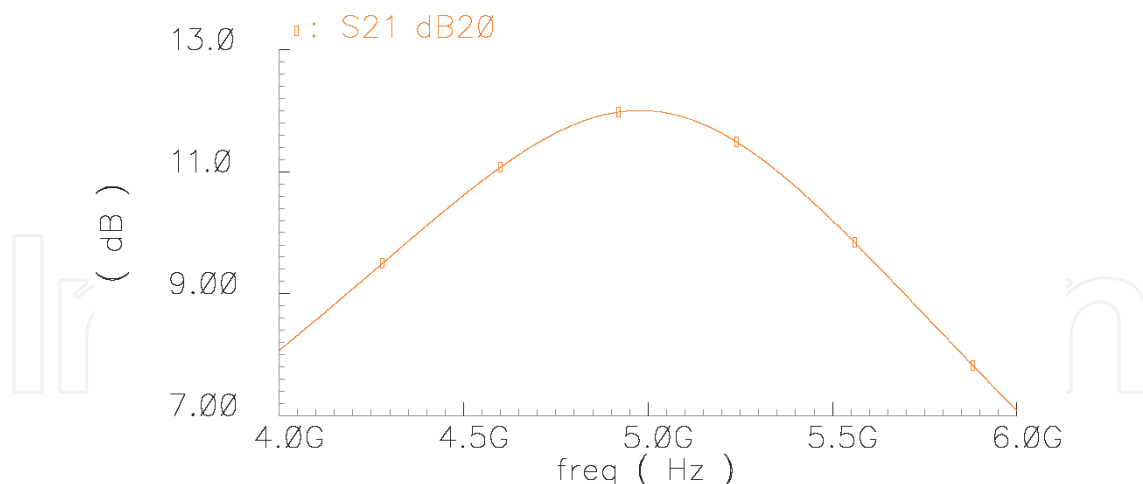


Fig. 12. S_{21} parameter of the circuit Fig. 8, in a dB chart.

4.1 Noise figure of a cascade system

Fig. 12 shows a cascade amplifying system, whose gain of each stage is A_i and the noise added by each stage is $N_{i-added}$.

The output noise due to the source is:

$$N_{o-source} = N_i \cdot A = N_i \cdot A_1 \cdot A_2 \cdot A_3 \quad (29)$$

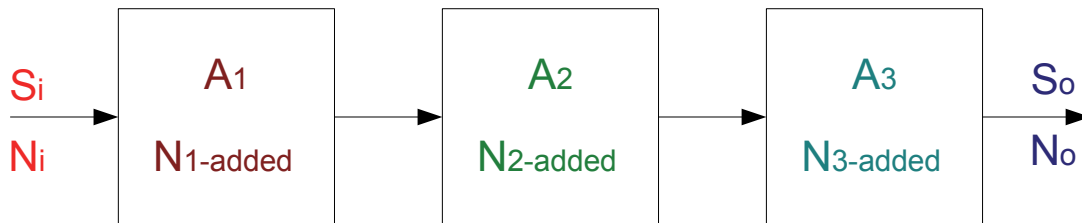


Fig. 13. Cascade amplifying system.

While the total output noise is:

$$N_o = N_i \cdot A_1 \cdot A_2 \cdot A_3 + N_{1\text{-added}} \cdot A_2 \cdot A_3 + N_{2\text{-added}} \cdot A_3 + N_{3\text{-added}} \quad (30)$$

which is the input noise multiplied by the gain of the three stages, plus the noise generated by the first stage and amplified by the stages 2 and 3, plus the noise generated by the second stage and amplified by the last stage, and plus the noise generated by the last stage.

Thus, combining expressions (29) and (30) into expression (25), the noise factor can be found as:

$$F = \frac{N_o}{N_{o\text{-source}}} = 1 + \frac{N_{1\text{-added}}}{N_i A_1} + \frac{N_{2\text{-added}}}{N_i A_1 A_2} + \frac{N_{3\text{-added}}}{N_i A_1 A_2 A_3} \quad (31)$$

This expression, with the aid of expression (27), can be re-written as:

$$F = F_1 + \frac{F_2 - 1}{A_1} + \frac{F_3 - 1}{A_1 A_2} \quad (32)$$

As can be observed from expression (32), the noise factor of the first stage is the most relevant to the total noise factor. That is the reason for putting most effort in the first stage in terms of noise minimization, thus requiring low noise amplifiers at the front of the system.

5. Conclusions

The basic knowledge of impedance matching between source and load, either with or without a transmission line is essential to the design of RF circuits. The analysis presented can be conducted by using Smith Charts and S-Parameters. The analysis in this chapter was oriented to RFID applications whereas other books provide general analysis.

6. References

- Kurokawa, K. (1965). Power Waves and the Scattering Matrix, *IEEE Trans. Microwave Theory and Tech.*, v.13, March 1965, pp. 194-202, ISSN 0018-9480.
- Lee, T. H. (2004). *The Design of CMOS Radio-Frequency Integrated Circuits - 2nd Edition*, Cambridge University Press, ISBN 0521835399.
- Rogers, J. & Plett, C. (2003) *Radio Frequency Integrated Circuit Design*, Artech House Inc, ISBN 1607839792.
- Coleman, C. (2004) *An Introduction to Radio Frequency Engineering*, Cambridge University Press, ISBN 0521834813.
- Razavi, B. (1998) *RF Microelectronics*, Prentice Hall, ISBN 0138875715.



Current Trends and Challenges in RFID

Edited by Prof. Cornel Turcu

ISBN 978-953-307-356-9

Hard cover, 502 pages

Publisher InTech

Published online 20, July, 2011

Published in print edition July, 2011

With the increased adoption of RFID (Radio Frequency Identification) across multiple industries, new research opportunities have arisen among many academic and engineering communities who are currently interested in maximizing the practice potential of this technology and in minimizing all its potential risks. Aiming at providing an outstanding survey of recent advances in RFID technology, this book brings together interesting research results and innovative ideas from scholars and researchers worldwide. Current Trends and Challenges in RFID offers important insights into: RF/RFID Background, RFID Tag/Antennas, RFID Readers, RFID Protocols and Algorithms, RFID Applications and Solutions. Comprehensive enough, the present book is invaluable to engineers, scholars, graduate students, industrial and technology insiders, as well as engineering and technology aficionados.

How to reference

In order to correctly reference this scholarly work, feel free to copy and paste the following:

Paulo Crepaldi, Tales Pimenta and Luis Ferreira (2011). Radio Frequency Background, Current Trends and Challenges in RFID, Prof. Cornel Turcu (Ed.), ISBN: 978-953-307-356-9, InTech, Available from: <http://www.intechopen.com/books/current-trends-and-challenges-in-rfid/radio-frequency-background>

INTECH
open science | open minds

InTech Europe

University Campus STeP Ri
Slavka Krautzeka 83/A
51000 Rijeka, Croatia
Phone: +385 (51) 770 447
Fax: +385 (51) 686 166
www.intechopen.com

InTech China

Unit 405, Office Block, Hotel Equatorial Shanghai
No.65, Yan An Road (West), Shanghai, 200040, China
中国上海市延安西路65号上海国际贵都大饭店办公楼405单元
Phone: +86-21-62489820
Fax: +86-21-62489821

© 2011 The Author(s). Licensee IntechOpen. This chapter is distributed under the terms of the [Creative Commons Attribution-NonCommercial-ShareAlike-3.0 License](#), which permits use, distribution and reproduction for non-commercial purposes, provided the original is properly cited and derivative works building on this content are distributed under the same license.

IntechOpen

IntechOpen